

Wavenumber interactions of turbulent boundary layer flow with structures exhibiting the acoustic black hole effect

Micah R. Shepherd, Philip A. Feurtado and Stephen C. Conlon

Citation: *Proc. Mtgs. Acoust.* **39**, 065002 (2019); doi: 10.1121/2.0001231

View online: <https://doi.org/10.1121/2.0001231>

View Table of Contents: <https://asa.scitation.org/toc/pma/39/1>

Published by the [Acoustical Society of America](#)

ARTICLES YOU MAY BE INTERESTED IN

[Wavenumber scattering and the interactions of turbulent boundary layer flow with the structures exhibiting the acoustic black hole effect](#)

The Journal of the Acoustical Society of America **146**, 2837 (2019); <https://doi.org/10.1121/1.5136833>

[Practical realisation of an active acoustic metamaterial building block](#)

Proceedings of Meetings on Acoustics **39**, 045006 (2019); <https://doi.org/10.1121/2.0001229>

[Improving mentored research relationships](#)

Proceedings of Meetings on Acoustics **39**, 025002 (2019); <https://doi.org/10.1121/2.0001251>

[Simulation of the pressure field beneath a turbulent boundary layer using realizations of uncorrelated wall plane waves](#)

The Journal of the Acoustical Society of America **140**, 1268 (2016); <https://doi.org/10.1121/1.4960516>

[Multi-objective optimization of acoustic black hole vibration absorbers](#)

The Journal of the Acoustical Society of America **140**, EL227 (2016); <https://doi.org/10.1121/1.4961735>

[Acoustic radiation force and torque on inhomogeneous particles in the Born approximation](#)

Proceedings of Meetings on Acoustics **39**, 045007 (2019); <https://doi.org/10.1121/2.0001255>



**Advance your science and career
as a member of the**

ACOUSTICAL SOCIETY OF AMERICA

LEARN MORE



178th Meeting of the Acoustical Society of America

San Diego, California

2-6 December 2019

Structural Acoustics and Vibration: Paper 2aSA5**Wavenumber interactions of turbulent boundary layer flow with structures exhibiting the acoustic black hole effect****Micah R. Shepherd***Applied Research Laboratory, The Pennsylvania State University, State College, PA, 16801;
mrs30@psu.edu***Philip A. Feurtado***Johns Hopkins University, Laurel, MD; Philip.Feurtado@jhuapl.edu***Stephen C. Conlon***The Pennsylvania State University, State College, PA; scc135@psu.edu*

Beam and plate-like structures with non-constant surface impedance are known to exhibit wavenumber scattering such that the wavenumber energy of a vibration mode of the structure is spread over a wide wavenumber band. The scattered energy can couple into partially-correlated forcing functions, such as turbulent boundary layer (TBL) flow, which exhibit a broadband wavenumber spectrum centered at the convective wavenumber. The overall effect is an increased amount of radiated noise for certain flow speeds. Recently, structures with embedded acoustic black holes (ABH) have shown good noise and vibration level reductions for point excitations. However, it will be shown that when excited by complex, partially-correlated forcing functions such as TBL flow, the wavenumber scattering caused by the power-law taper of the ABH can lead to increased radiated noise levels. The flow speed and wavenumber dependence of the TBL/ABH interactions will be presented using dimensional analysis.

1. INTRODUCTION

The acoustic black hole (ABH) effect occurs when a structure exhibits a power-law taper such that the wavespeed slows and amplitude increases as the thickness in the taper decreases [1,2]. When damping material is added to the taper, the energy in the taper can be dissipated to overcome reflections from a non-infinite taper length. Good vibration reduction has been achieved for beams and plates with imbedded ABHs when excited by a point force [3-5] or diffuse field [6]. This paper illustrates the impact of turbulent boundary layer (TBL) flow exciting plates with an imbedded array of ABHs. It is shown that the wavenumbers of the TBL excitation can couple with imbedded ABHs such that vibration and noise levels of the ABH plate can be higher than that of the uniform plate under certain flow speeds.

2. TURBULENT BOUNDARY LAYER FLOW

The partial correlation of the pressures created by TBL flow was characterized by Corcos [7] as a force cross-spectral density matrix.

$$G_{FF} = \varphi_p \{ e^{-\alpha_x |\omega \xi_x / U_c|} e^{-\alpha_y |\omega \xi_y / U_c|} e^{j\omega \xi_x / U_c} \} \quad (1)$$

In Eq. 1, α_x and α_y are the decay coefficients in the streamwise and spanwise directions respectively, ξ is the separation distance in both directions, ω is the angular frequency, U_c is the convective speed (approximated as 70% of the freestream velocity) and φ_p is the pressure autospectrum. In the streamwise direction, the TBL force spectrum is a decaying oscillation. A convective wavenumber k_c can be defined as the angular frequency divided by the convective speed.

Equation 1 can be transformed into the wavenumber domain to obtain the wavenumber sensitivity function as shown in Fig. 1. The sensitivity function is normalized by φ_p while the wavenumber is normalized by the convective wavenumber. The TBL force peaks when the wavenumber equals the convective wavenumber, with the region surrounding it often referred to as the convective ridge. Above the convective wavenumber, the TBL force rapidly drops in amplitude. Below it, the TBL force approaches a constant. The wavenumber characteristics of TBL flow is discussed in more detail by Bonness *et. al* [11].

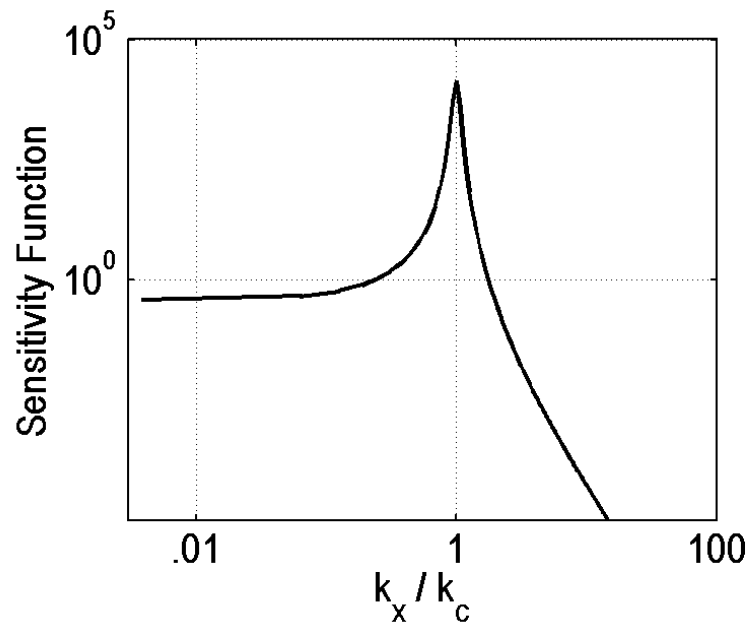


Figure 1. The wavenumber sensitivity function of the Corcos TBL model, normalized by the convective wavenumber.

Since the convective wavenumber depends on the convective speed, the convective ridge will also shift with speed. Fig. 2 shows a representation of the wavenumber sensitivity function as a function of convective speed and wavespeed. Since wavespeed is inversely proportional to wavenumber, the low wavenumber region of the sensitivity function is on the right while the high wavenumber region is on the left. Four classes of vehicles are also labeled in Fig. 2 according to their nominal operating speeds. The convective ridge is shown in dark red and illustrates how vehicle speed impacts the sensitivity function of the TBL force. The boxed region represents an approximate range of wavespeeds that may be typical for materials used in these vehicles. When the convective ridge falls within this range, strong coupling will occur between the force and the structure.

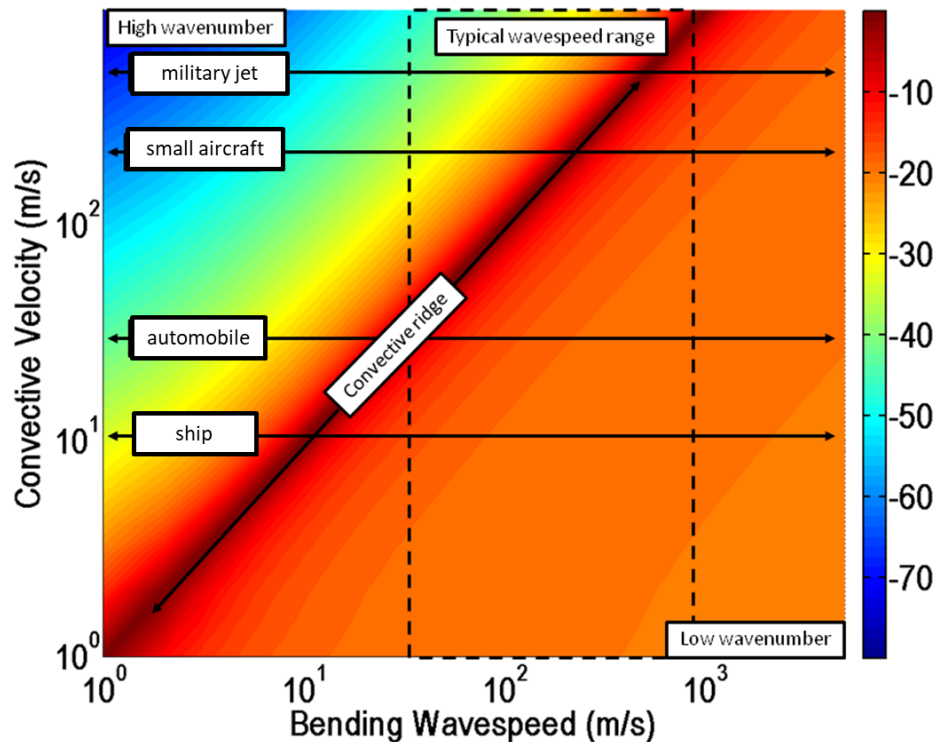


Figure 2. The wavenumber sensitivity as a function convective velocity and wavespeed. The dotted box region illustrates normal ranges of structural wavespeeds for these vehicles. Strong coupling would be expected between the forcing function and the structure when the convective ridge falls within the dotted box. The color contour is the sensitivity function (dB re 1).

3. WAVENUMBER INTERACTIONS

A. FINITE ELEMENT MODEL

A finite element model of a flat plate (0.857 m x 0.854 m x 3.3 mm) was created to examine the vibration and radiated noise from TBL flow from three flow speeds [8]. The plate contains a 5x4 grid of imbedded ABHs with a taper power of 2.2 while the truncation thickness of each ABH is 0.26 mm and the diameter is 10 cm. The material properties of the plate are listed at the bottom of Table 1. The first sets of ABH modes cut on around 1.7 kHz. The mesh was composed of quadratic hexahedral elements and stiff springs were used as boundary conditions at the edges. A lumped parameter procedure was used to compute the radiated noise of the plate when placed in a rigid, infinite baffle [9].

Table 1. (top) Parameters of the imbedded ABH array. (bottom) Material properties.

Taper Power	Truncation Thickness	Diameter	Array
2.2	0.26 mm	10 cm	5 x 4

Material	Youngs Modulus	Density	Poisson's Ratio	Loss Factor
Aluminum	70.0 GPa	2700 kg/m ³	0.35	0.0001
3M ISODAMP TD-1604	0.009 GPa	1812 kg/m ³	0.45	0.2

B. LENGTH SCALE MATCHING

The plate will have two bounding thicknesses: the standard flat plate thickness and the ABH minimum thickness. These two values will define bounding critical frequencies. A convective coincidence frequency can also be computed using the convective speed, U_c instead of the acoustic wavespeed:

$$f_{conv} = \frac{U_c^2}{2\pi} \sqrt{\frac{\rho h}{D}}, \quad (3)$$

where ρ is the mass density, D is the flexural rigidity and h is the plate thickness. The critical frequency and convective coincidence frequencies are shown for three different flow speeds in Table 2. Each speed represents a different class of vehicle. Since the slowest speed would be from a ship, water was used as the external fluid. The ratio of the critical to convective coincidence frequency is also shown the table. When the ratio is small, the length scales of the TBL pressures are much smaller than the wavelengths of acoustic waves. When the ratio is near unity, the length scales of the TBL pressure are close to the acoustic wavelength. A structural additional length scale will also come into play from wavelengths of the ABH modes.

Table 2. The critical frequency and convective coincidence frequency for three different flow speeds

	Flow Speed	Critical Frequency (thick / thin)	Convective Coincidence (thick / thin)	Ratio	Ext. Fluid
Ship	5 m/s	69.2 / 878 kHz	0.40 / 5.1 Hz	5.75e-6	Water
Fast Automobile	44 m/s	3.62 / 45.9 kHz	30.1 / 381.9 Hz	0.0083	Air
Commercial Aircraft	216 m/s	2.86 / 36.3 kHz	702.7 / 8919 Hz	0.246	Air (35,000 ft)

C. RESULTS – SHIP, AUTOMOBILE, AIRCRAFT

The surface-averaged velocity and the radiated sound power are shown from 10 – 10,000 Hz in Figure 3 for the panel excited by flow at the nominal speed of a ship, 5 m/s. Fluid loading is accounted for as if the panel were submersed in water. The uniform plate is shown along with the damped and undamped ABH plate. At low frequencies, a shift in the first natural frequencies of the plate is seen along with a small increase in amplitude for the ABH plate. As more resonance peaks are excited and the modal density increases, the response of the ABH plate drops below the uniform plate. At higher frequencies (>800 Hz), the vibration of the three panels is similar while the radiated noise of the uniform plate is higher than for the ABH plates. The lower radiation is due to a reduction in radiation efficiency of the plate with the addition of the ABHs [3].

Figure 4 (left) shows the average wavenumber spectrum computed using the two-dimensional Fourier transform [10] for the plate response at the 2 kHz one-third octave band. Extensive wavenumber scattering is seen for ABH plates (B & C) as compared to the uniform plate (A). This is caused by the wavespeed changes which occur within the ABHs. The TBL forcing function (D) is nearly constant over the relevant wavenumber range since it is operating well below the convective ridge for flow at this speed. On the right of Figure 4, the wavenumber relationship is shown as a function of frequency for the uniform thickness plate, minimum ABH thickness using infinite plate theory. The acoustic and convective wavenumber curves are also shown. The region between these uniform (red) and minimum thickness (black) curves represents the wavenumber sweep that occurs for the ABH plates. The frequency range where the convective ridge passes through the ABH sweep is below 10 Hz. Since no local or global modes occur at this low of frequency, the TBL wavenumbers do not interact with the uniform or ABH structure. At higher frequencies, the differences in the wavenumber content between the uniform and ABH plates are negligible.

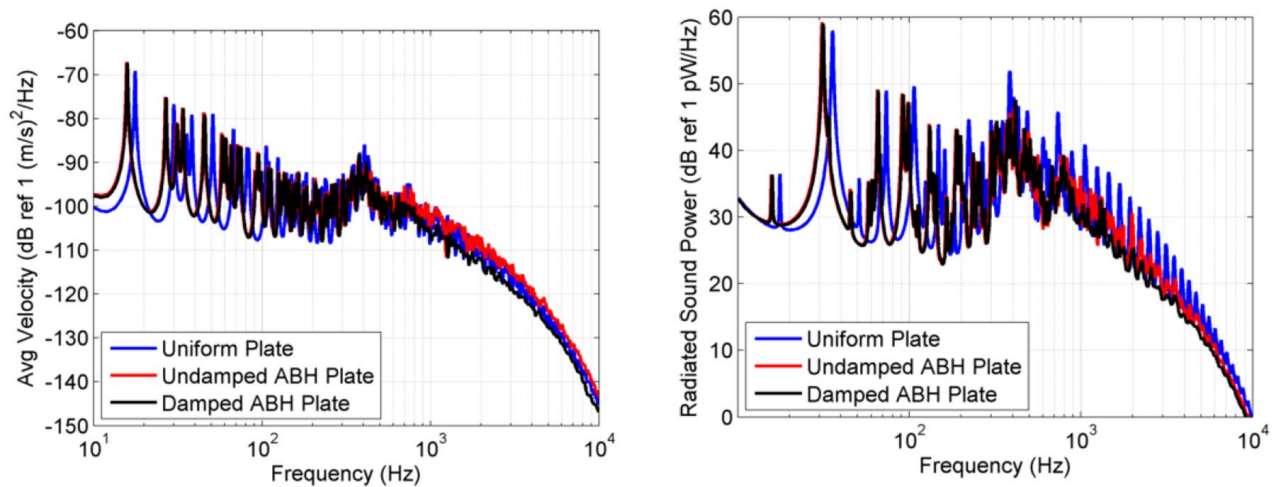


Figure 3. Surface-averaged velocity (left) and radiated sound power (right) of the panel excited by flow at 5m/s in water.

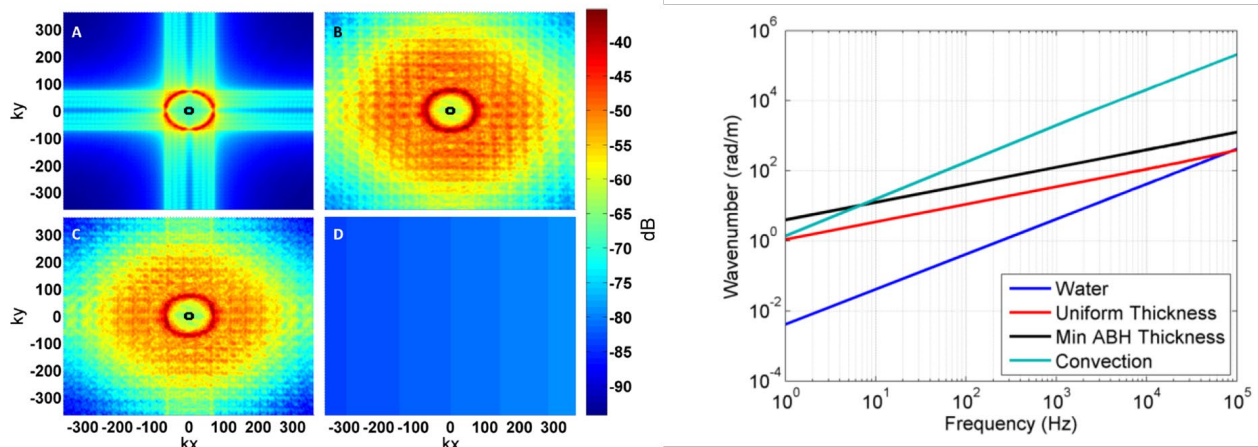


Figure 4. (Left) Average wavenumber spectrum of the uniform plate (A), undamped ABH plate (B), damped ABH plate (C) and TBL forcing function (D) at the 2 kHz one-third octave band (5 m/s flow). The radiation circle is also shown as a black circle near the center of A, B and C (Right) Bending wavenumber curves are shown using infinite plate theory as a function of frequency and compared with acoustic and convective wavenumbers.

For TBL flow excitation from a fast automobile, the story begins to change. Figure 5 shows the velocity and sound power for the panel excited by 44 m/s flow (in air). At very low frequencies, there are only subtle difference between the three plates. Around 100 Hz, the velocity and sound radiation are slightly higher for the

ABH plates. Above 2 kHz, the velocity of the undamped ABH plate is slightly higher than that of the uniform plate while the damped ABH plate levels are slightly below the uniform plate. The radiated noise levels are highest for the undamped ABH plate for but then fall below the uniform and then the two levels match. The damped ABH plate noise is lower for all frequencies above 2 kHz.

Figure 6 (left) shows the average wavenumber spectrum for the plate response at 2.5 kHz one-third octave band with the corresponding radiation circle in black. Extensive wavenumber scattering is again seen for ABH plates (B & C) as compared to the uniform plate (A). The TBL forcing function (D) is slowly increasing as wavenumber increases but is still below the convective ridge. On the right of Figure 4, the convective wavenumber is shown to cross through the ABH wavenumber sweep between approximately 70 – 300 Hz. This causes a small increase in vibration and noise for the ABH plates. Additional wavenumber interactions occur for the ABH plate at higher frequency due to the existence of localized ABH modes. Also, the critical frequency is now within the frequency range of interest and the structure enters the supersonic realm above 3.6 kHz for the uniform plate.

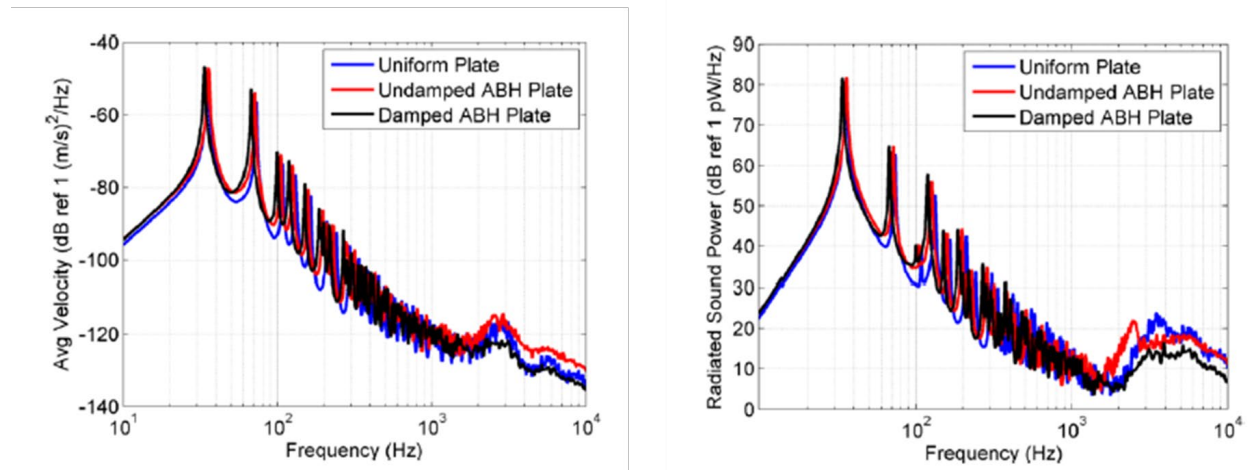


Figure 5. Surface-averaged velocity (left) and radiated sound power (right) of the panel excited by flow at 44 m/s (in air).

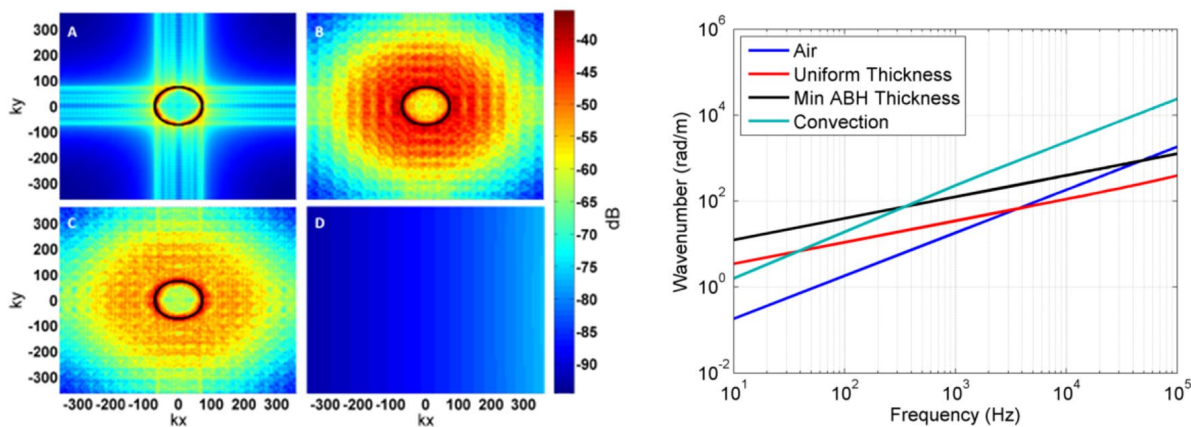


Figure 6. (Left) Average wavenumber spectrum of the uniform plate (A), undamped ABH plate (B), damped ABH plate (C) and TBL forcing function (D) at the 2.5 kHz one-third octave band (44 m/s flow). The radiation circle is also shown as a black circle near the center of A, B and C (Right) Bending wavenumber curves are shown using infinite plate theory as a function of frequency and compared with acoustic and convective wavenumbers.

For flow excitation at speeds for a commercial aircraft, the vibration and noise levels now increase significantly for the ABH plate at high frequencies, as shown in Figure 7. The damped ABH plate is still able to decrease the levels from the undamped ABH plate but not enough to fall below the levels of the uniform plate. Figure 8 shows the average wavenumber spectrum for the 4 kHz third octave band with high energy levels seen near the convective ridge. Wavenumber interactions now occur since the convective ridge falls within the operating ABH wavenumber sweep. Physically, this exists because the ABH modal frequencies fall in the same frequency range where the convective ridge occurs, allowing for efficient coupling to occur between the length scales of the forcing function and the modes of the ABH. Thus the energy acceptance increases for the ABH plates such that they are noisier than the uniform plate, despite the use effective use of damping.

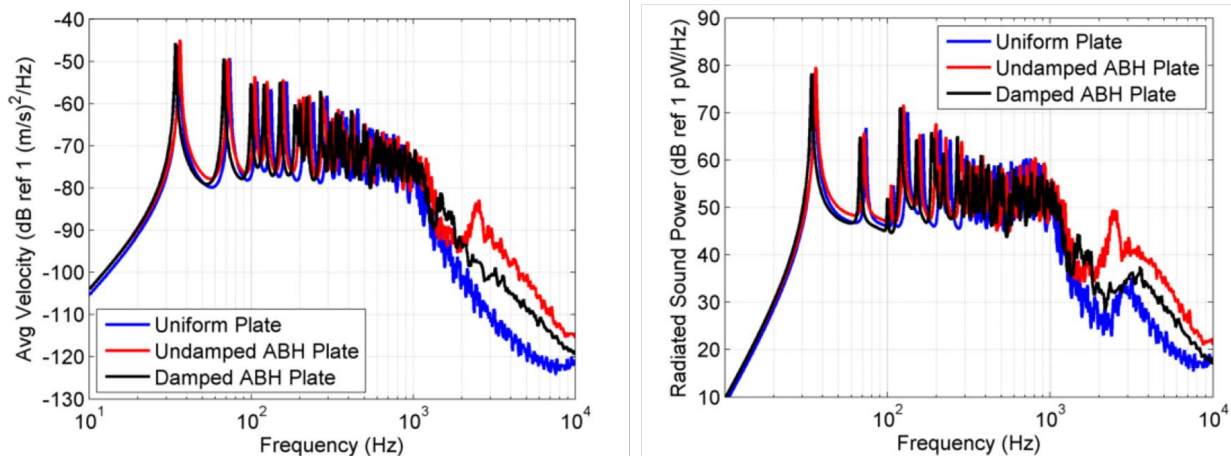


Figure 7. Surface-averaged velocity (left) and radiated sound power (right) of the panel excited by flow at 216 m/s (in air at 35,000 ft).

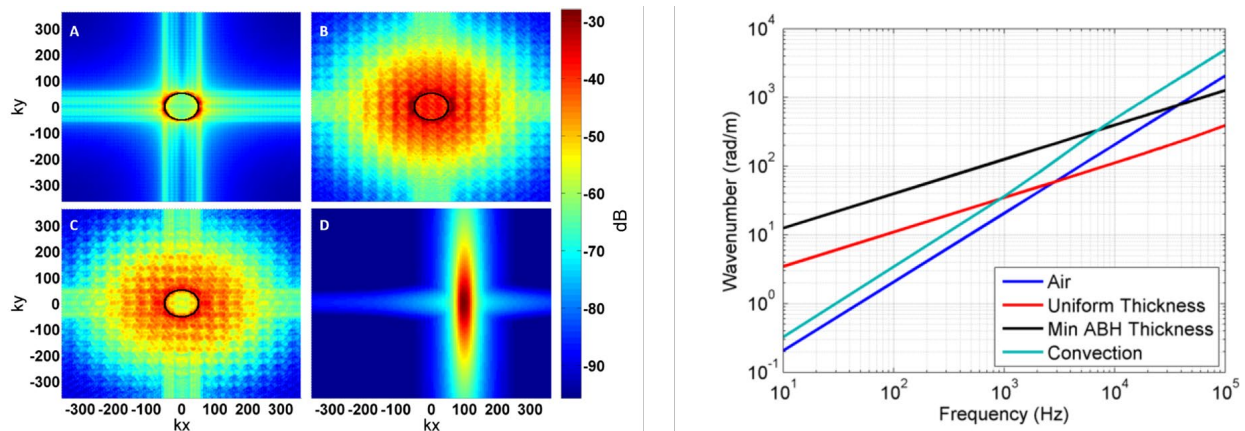


Figure 8. (Left) Average wavenumber spectrum of the uniform plate (A), undamped ABH plate (B), damped ABH plate (C) and TBL forcing function (D) at the 4 kHz one-third octave band (216 m/s flow). The radiation circle is also shown as a black circle near the center of A, B and C (Right) Bending wavenumber curves are shown using infinite plate theory as a function of frequency and compared with acoustic and convective wavenumbers.

4. CONCLUSIONS

Wavenumber interactions can occur between TBL flow and imbedded ABH vibration absorbers when the cut-on frequency of the ABH modes are near the frequency of the convective ridge. The inclusion of ABH vibration absorbers on a plate may increase this interaction and cause vibration and noise radiation levels to increase. This is most likely to occur for higher speed flow but will depend of the structural thickness, ABH parameters and frequency range of interest. This effect has not previously been observed since only single point excitation have been considered without flow.

REFERENCES

- ¹ M. Mironov, "Propagation of a flexural wave in a plate whose thickness decreases smoothly to zero in a finite interval," *Sov. Phys. Acoust.* **34** (1988).
- ² V. Krylov and F. Tilman "Acoustic black holes for flexural waves as effective vibration dampers," *J. Sound Vib.* **274** (2004).
- ³ S.C. Conlon, J.B. Fahnlne, and F. Semperlotti "Numerical analysis of the vibroacoustic properties of plates with embedded grids of acoustic black holes," *J. Acoust. Soc. Am.* **137** (2015).
- ⁴ C.A. McCormick and M.R. Shepherd, "Design optimization and performance comparison of three styles of acoustic black hole vibration absorbers," *J. Sound Vib.* **470** (2020).
- ⁵ P.A. Fuertado and S.C. Conlon, "An Experimental investigation of acoustic black hole dynamics at low, mid and high frequency," *J. Vib. Acoust.* **138** (2016).
- ⁵ P.A. Fuertado and S.C. Conlon, "Transmission loss of plates with embedded acoustic black holes," *J. Acoust. Am.* **138** (2017).
- ⁷ G.M. Corcos "Resolution of pressure in turbulence," *J. Acoust. Soc. Am.* **35** (1963).
- ⁸ P.A. Fuertado "Quiet Structure Design Using Acoustics Black Holes," PhD dissertation (2017).
- ⁹ J.B. Fahnlne and G.H. Koopmann, "A lumped parameter model for the acoustic power output from a vibrating structure," *J. Acoust. Soc. Am.* **100** (1996).
- ¹⁰ O. Robin, A. Berry, N. Atalla, S.A. Hambric and M.R. Shepherd, "Experimental evidence of modal wavenumber relation to zeros in the wavenumber spectrum of a simply supported plate," *J. Acoust. Soc. Am.* **137** (2015).
- ¹¹ W.K. Bonness, John B. Fahnlne, Peter D. Lysak and M.R. Shepherd, "Modal forcing function for structural vibration from turbulent boundary layer flow," *J. Sound Vib.* (2017).